Int. J. Electrochem. Sci., 16 **(2021)** Article Number: 211037, doi: 10.20964/2021.10.45

International Journal of
ELECTROCHEMICAL
SCIENCE
www.electrochemsci.org

A Coupled Electro-Chemo-Mechanical Model for Li-ion Batteries: Effect of Stress on the Voltage Hysteresis of Lithium Ion Batteries

Pengfei Yu[1,2], *Junwen Xiao*[1], *Hai Hu*[1], *Mingju Lin*[1], *and Yaohong Suo* [1,*]

[1] School of Mechanical Engineering and Automation, Fuzhou University, Fuzhou, 350108, China
[2] State Key Laboratory for Strength and Vibration of Mechanical Structures, School of Aerospace, Xi'an Jiaotong University, Xi'an 710049, People Republic of China
[*]E-mail: yaohongsuo@126.com

Received: 2 July 2021 / *Accepted:* 9 August 2021 / *Published:* 10 September 20211

Experiments have shown that stress has a significant effect on the hysteresis loop of the electrode potential while charging or discharging Li-ion batteries. In this work, considering the influence of stress on lithium-ion diffusion and electrode potential, a fully coupled electro-chemo-mechanical model is developed in a spherical electrode particle under galvanostatic operation. Then, some simulations are carried out to investigate the distribution of lithium-ion concentration, diffusion-induced stresses and electric potential. Meanwhile, the influences of C-rate and electrode particle radius are also discussed. Numerical results show that the smaller C-rate and electrode particle radius are beneficial in reducing the diffusion-induced stresses and improving the effective capacity of Li-ion batteries. Finally, some comparisons of lithium-ions concentration and the hysteresis of electrode potential between the present model and Jin's model (without the effect of deformation on diffusion) are performed. The work can provide some tips for designing electrodes in Li-ion batteries with a high capacity and durability.

Keywords: Voltage hysteresis; Diffusion-induced stress; Electro-chemo-mechanical model; Lithium-ion batteries

1. INTRODUCTION

Lithium-ion batteries (LIBs) have become indispensable electrochemical energy storage devices due to their higher energy density and longer life [1, 2]. During the process of charge and discharge in LIBs, the electrode is usually accompanied with volume deformation [3, 4] and the diffusion-induced stress (DIS) [5]. Excessive stress may lead to the electrode failure and cause the electrochemical performance degradation by altering the electrode potential. Therefore, the challenge

for high-performance LIBs is not only a chemical problem, but also a mechanical one. Thus, it is essential to investigate the evolution of DIS to improve the electrochemical performance and cycle lifetime of LIBs.

There is extensive research on the coupled diffusion-stress model to understand the influence of DIS on loss of capacity and life expectancy. Prussin [5] first deduced the diffusion-induced stress in Si wafers by adopting the method similar to the thermal stress. Zhang [6] investigated the diffusion-induced stress in the electrode particles of various shapes and sizes. Zhao [7] outlined a theory to study how particle size and C-rate affect electrode fracture in LIBs. Cheng and Verbrugge [8] took into account the effect of surface tension and surface modulus on DIS within spherical nanoparticles, and revealed that both the magnitude and distribution of stresses can be significantly affected by surface mechanics if the particle diameter is in the nanometer range. Suo and Yang [9] developed a one-dimensional fully coupled reaction-diffusion-stress model with the influence of the local solid reaction. Using gradient material and considering the contribution of chemical reaction, Hu [10] developed a generalized diffusion-deformation-reaction coupling model under potentiostatic operation. Li [11] established a chemo-mechanical model for the lithiation-induced deformation of a-Si electrode from the frameworks of phase-field theory and viscoplastic constitutive relationship. These works mentioned above mainly focused on the chemo-mechanical behavior in lithium-ion battery electrodes and they were one-way coupling or intercoupling. However, the influence of diffusion-induced stress on the electrical properties is not taken into account.

Some experiments suggest that stress can impact the potential of the electrode during charging and discharging. For example, Sethuraman [12] pointed out that stress had a significant effect on the open-circuit electric potential of the silicon electrode by experimental observation. Piper [13] attributed the impediment of lithiation to the increase of elastic energy, and provided a qualitative explanation to their experiment. However, the explanation can only be applied to the electrodes in an equilibrium state. In the operation of LIBs, the evolution of electrode voltage versus capacity is different during the charge and discharge, and thus forms a hysteresis loop, which is called voltage hysteresis [14]. Bower [15] incorporated stress effects into the electrochemical reactions and established a continuum model of deformation, diffusion, stress, electrochemical reactions and electrostatic fields in a Li-ion half-cell. Lu [14] proposed a modified Butler-Volmer equation which includes the influence of mechanical stresses on the voltage hysteresis in the electrodes of LIBs. Song [16] indicated that the effects of the stress on the voltage hysteresis depended on the material's property, charge rate and electrode size. Effects of surface stresses of nanoparticles and interparticle compressions on the voltage hysteresis of lithium ion batteries were investigated by Jin [17]. Peng [18] developed a reaction-diffusion-stress coupled model to discuss the stress induced voltage hysteresis under potentiostatic operation. A coupled mechanics-electrochemistry formalism for solid polymer electrolyte was developed by Hao [19] to address the effect of stress on the electrochemical performance. The stress-potential coupling of electrode materials was investigated in these above studies, however the effect of stress on the diffusion is neglected, thus they are not fully coupled.

Deformation (stress) plays an important role in the diffusion of lithium ions, as experiments [20-22] have confirmed. Moreover, it can also affect the electrode potential. At present, there are few reports of the full diffusion-electro-mechanical coupling. The present paper will consider the influence

of the deformation on the lithium diffusion and electrode potential, take a spherical silicon electrode particle as an object and develop an electro-chemo-mechanical coupling model to discuss the evolution of Li-ions concentration, DIS and electrode potential under galvanostatic operation. Then, numerical simulations are performed to capture the impact of C-rate and particle size on DIS and electrode potential. The proposed model can be used to analyze electrode degradation behaviours and provide design guidance to improve effective PFR capability of LIBs.

2. MODEL FORMULATION

The schematic of a spherical electrode particle with the radius r_0 is shown in Fig. 1.

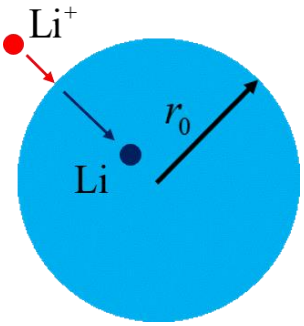

Figure 1. Schematic of a spherical electrode particle

2.1 Butler-Volmer electro-chemical reaction

At the interface between the active electrode material and the electrolyte, the electrochemical reaction of the lithium ions and the active electrode material occurs as follows.

$$\mathrm{A} + x\mathrm{Li}^+ + x\mathrm{e}^- \underset{k_c}{\overset{k_a}{\rightleftharpoons}} \mathrm{Li}_x\mathrm{A}, \qquad (1)$$

where Li^+ and A are lithium-ions and active materials respectively. k_a and k_c are reaction rate constants for anodic reaction and cathodic reaction, respectively.

Based on the modified Butler-Volmer equation [14], the electro-chemical reaction velocity affected by the electrode potential and the hydrostatic pressure at the surface of electrode is written as

$$i_n = i_0 \left\{ \exp\left[(1-\alpha) \frac{F\left(E_V - E_{eq}\right) - \sigma_h^s \Omega}{R_g T} \right] - \exp\left[-\alpha \frac{F\left(E_V - E_{eq}\right) - \sigma_h^s \Omega}{R_g T} \right] \right\}, \qquad (2)$$

where i_n, i_0, α, F, R_g, T, Ω and σ_h^s represent the net current density, the exchange current density, charge transfer coefficient, Faradic constant, universal gas constant, absolute temperature, partial molar volume and hydrostatic pressure at the electrode surface. E_V is the electrode potential and E_{eq} is the potential at the equilibrium state of the whole electrode. $E_V - E_{eq}$ is the overpotential that signifies the degree to deviate from equilibrium state. The electrochemical reaction of lithium-ions across the solid-liquid interface is impacted by the mechanical stresses. The mechanical compression

in the surface layer would impede the intercalation of lithium into the cathodic materials. $-\sigma_h^s\Omega$ represents the energy barrier induced by mechanical work for isotropic materials, reflecting that lithium-ions intercalation into the solid-liquid interface need to overcome the impeding from surface mechanical stresses. The exchange current density i_0 can be written as

$$i_0 = Fk_0 c_{\mathrm{Li}^+}^{1-\alpha}\left(c_{\max}-c_s\right)^{1-\alpha} c_s^{\alpha}, \qquad (3)$$

where k_0, c_{Li^+}, c_s and $c_{\max}$ are the reaction rate constant at equilibrium state, lithium concentration in the electrolyte, the lithium concentration at the electrode surface and the maximum lithium concentration in the active material, respectively.

The electrode potential can be solved from Eq. (2) under the assumption of $\alpha = 0.5$

$$E_V = \frac{2R_gT}{F}\operatorname{arcsinh}\left(\frac{i_n}{2i_0}\right)+\frac{\sigma_h^s\Omega}{F}+E_{eq}. \qquad (4)$$

It is pointed out that $i_n < 0$ means lithiation while $i_n > 0$ stands for delithiation in Eq. (4). The first term in the right of Eq. (4) represents the overpotential that drives the electrochemical reaction, and the second one is the overpotential caused by the diffusion-induced stress.

According to the fitting result of Sethuraman [12], the equilibrium potential is given as follows

$$E_{eq} = -4.76Q^6 + 9.34Q^5 - 1.8Q^4 - 7.13Q^3 + 5.8Q^2 - 1.94Q + 0.62,\ 0 \le Q \le 1, \qquad (5)$$

where $Q = 3\int_0^{r_0} r^2 c\mathrm{d}r \Big/ \left(c_{\max} r_0^3\right)$ is a dimensionless capacity, and r is the radius.

2.2 Mechanical equations

Similar to the thermal strain, the relationship of stress and strain with diffusion induced deformation is written as [6]

$$\begin{aligned}\varepsilon_r &= \frac{1}{E}\left(\sigma_r - 2\nu\sigma_\theta\right)+\frac{\Omega}{3}c,\\ \varepsilon_\theta &= \frac{1}{E}\left[\sigma_\theta - \nu\left(\sigma_r+\sigma_\theta\right)\right]+\frac{\Omega}{3}c,\end{aligned} \qquad (6)$$

where ε_r, ε_θ, σ_r, σ_θ, E and ν are the radial strain, hoop strain, radial stress, hoop stress, Young's modulus and Poisson's ratio, respectively. c is the concentration of lithium-ions in the electrode.

Based on the linear elastic theory and small deformation assumption, the strain-displacement relationship in the spherical coordinate system is as follows

$$\varepsilon_r = \frac{\partial u}{\partial r},\ \varepsilon_\theta = \frac{u}{r}, \qquad (7)$$

where u is the radial displacement.

The equilibrium equation neglecting body forces in the spherical electrode can be written as

$$\frac{\partial\sigma_r}{\partial r}+\frac{2}{r}\left(\sigma_r-\sigma_\theta\right)=0. \qquad (8)$$

Substituting Eqs. (6) and (7) into Eq. (8), the mechanical equilibrium equation can be expressed as

$$\frac{\partial^2 u}{\partial r^2}+\frac{2}{r}\frac{\partial u}{\partial r}+\frac{2u}{r^2}=\left(\frac{1+\nu}{1-\nu}\right)\frac{\Omega}{3}\frac{\partial c}{\partial r}. \qquad (9)$$

Assume that there is no initial deformation of the electrode particle and that there is no stress at the surface. Additionally, the displacement at the center of sphere is zero due to the symmetry. Thus, the initial and boundary conditions can be written as

$$\begin{aligned} &u\big|_{t=0}=0,\\ &u\big|_{r=0}=0,\ \sigma_r\big|_{r=r_0}=0. \end{aligned} \qquad (10)$$

2.3 Diffusion equation

The electrochemical potential μ, in an ideal solid solution can be written as [23, 24]

$$\mu=\mu_0+R_gT\ln c-\Omega\sigma_h, \qquad (11)$$

where μ_0 is the chemical potential in a given standard state, R_g is the universal gas constant, and $\sigma_h=\left(\sigma_r+2\sigma_\theta\right)/3$ is the hydrostatic pressure.

The diffusion flux J and the electrochemical potential satisfy the following relationship

$$J=-Mc\frac{\partial\mu}{\partial r}=-\frac{Dc}{R_gT}\frac{\partial\mu}{\partial r}, \qquad (12)$$

where M is the mobility of lithium in the solid, and $D=MR_gT$ is the diffusion coefficient.

Supposing that the lithium-ions diffuse only along the radial direction, the diffusion equation abides by the mass conservation equation, i.e.,

$$\frac{\partial c}{\partial t}+\frac{1}{r^2}\frac{\partial}{\partial r}\left(r^2J\right)=0. \qquad (13)$$

Combining Eqs. (11)-(13), one can obtain

$$\frac{\partial c}{\partial t}=\frac{1}{r^2}\frac{\partial}{\partial r}\left[r^2D\left(\frac{\partial c}{\partial r}-\frac{\Omega c}{R_gT}\frac{\partial\sigma_h}{\partial r}\right)\right], \qquad (14)$$

where t is time. It should be noted that the stress coupling effect is considered not only in the diffusion equation (14) but also in the electrochemical reaction (4).

Given that the initial concentration of lithium-ions in the electrode is zero. Galvanostatic or potentiostatic operation takes place during charging or discharging. Only the galvanostatic operation is discussed in this work, which means that diffusion flux is constant at the surface of the electrode during the charge or discharge. Due to the symmetry of sphere, the diffusion flux at the center should be zero. Thus, the initial and boundary conditions for the diffusion should be given by

$$\begin{aligned} &c\big|_{t=0}=0,\\ &J\big|_{r=0}=0,\ J\big|_{r=r_0}=\frac{i_n}{F}. \end{aligned} \qquad (15)$$

Under galvanostatic operation, the net current density in the spherical particle is given as follow [16]

$$i_n=\frac{n_cc_{\max}Fr_0}{10800} \qquad (16)$$

where n_c is the value of C-rate. The net current density is determined from the C-rate and the radius of spherical electrode particle.

It can be derived from these above equations that Eqs. (4), (9) and (14) constitute the fully coupled electro-chemo-mechanical model equations. If the hydrostatic pressure disappears, the fully coupled model will reduce to Jin's model [17].

3. NUMERICAL RESULTS AND DISCUSSION

In order to discuss the evolution of the concentration, stresses and electrode potential in the spherical electrode particle, the electrode material is assumed to be silicon, and its parameters used in numerical simulation are listed in Table 1.

Table 1. Parameters used in numerical simulation.

Parameter	Value	Units
E	100 [17]	GPa
ν	0.27 [17]	/
Ω	4.26×10^{-6} [17]	$\mathrm{m^3/mol}$
D	2×10^{-16} [17]	$\mathrm{m^2/s}$
$c_{\max}$	3.13×10^{5} [17]	$\mathrm{mol/m^3}$
$c_{\mathrm{Li^+}}$	1000 [14]	$\mathrm{mol/m^3}$
k_0	10^{-12} [14]	$\mathrm{m^{2.5}/\left(mol^{0.5}\cdot s\right)}$
R_g	8.314	$\mathrm{J/\left(mol\cdot K\right)}$
T	293.15	K
r_0	500	nm

Figure 2 shows the distribution of lithium-ion concentration, radial stress, hoop stress, hydrostatic pressure and voltage hysteresis of the electrode, respectively, for electrode particle radius $r_0 = 500$ nm and C-rate $n_C = 1\,\mathrm{C}$. In Figs. 2(a), (b) and (c), the solid lines with symbol represent the charging process and the dotted lines with symbol stand by the discharge process.

Under galvanostatic operation, Fig. 2(a) and (b) describe the concentration distribution of lithium-ions with r/r_0 at lower dimensionless capacity and higher dimensionless capacity respectively. Lithium ions spread from the surface to the centre. Concentration at a fixed position will increase with time of charging. During the discharge, the concentration at the center is higher than that at the surface of the electrode, and the concentration gradually decreases with the increase of r/r_0. If the discharge time is longer, the concentration in a fixed position decreases because more lithium-ions are discharged.

Fig. 2(c) and (d) plot the distributions of the radial stress and hoop stress, respectively. The

radial stress is tensile during the charge while it is compressive during the discharge. The magnitude of the maximum radial stress occurs at the center of the sphere no matter whether the electrode is in charge or discharge. The radial stress is tensile during the charge and compressive during the discharge, while the hoop stress changes from tensile to compressive with increasing dimensionless r/r_0 during the charge and vice versa during the discharge. These variation trends of the radial and hoop stress can also be observed in [25]. The maximum hoop stress generates at the center no matter whether the battery is in charge or discharge.

Fig. 2(e) illustrates the variation of hydrostatic pressure at the surface of the electrode particle with the dimensionless capacity Q. From Fig. 2(e), it can be found that the hydrostatic pressure is compressive during the charge while it is tensile during the discharge. In addition, the magnitude of hydrostatic pressure increases with the decrease of Q during the discharge, whereas it quickly increases at the beginning of charge and then decreases up to the steady (constant) with the increasing of dimensionless capacity Q as the charge continues. The variation trend of the hydrostatic pressure $\sigma_h=(\sigma_r+2\sigma_\theta)/3$ at the electrode surface is consistent with that in Fig. 2(c) and (d), which can be further proved in [14, 25]. The curve of hydrostatic pressure forms a hysteresis loop during lithiation and delithiation.

The variation of the electrode potential with the non-dimensional capacity Q is shown in the Fig. 2(f) during the process of charge and discharge. The electrode potential gradually reduces as Q increases during the charge. When the potential is zero, the charge is completed. The potential of the electrode gradually increases with the reduction of Q during discharging. Similar to the hydrostatic pressure, the variation of the electrode potential also forms a hysteresis loop during lithiation and delithiation.

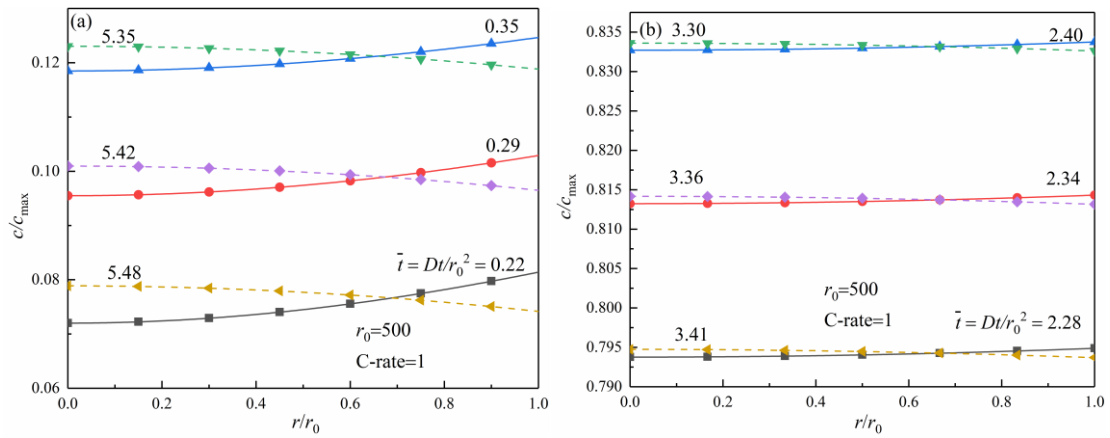

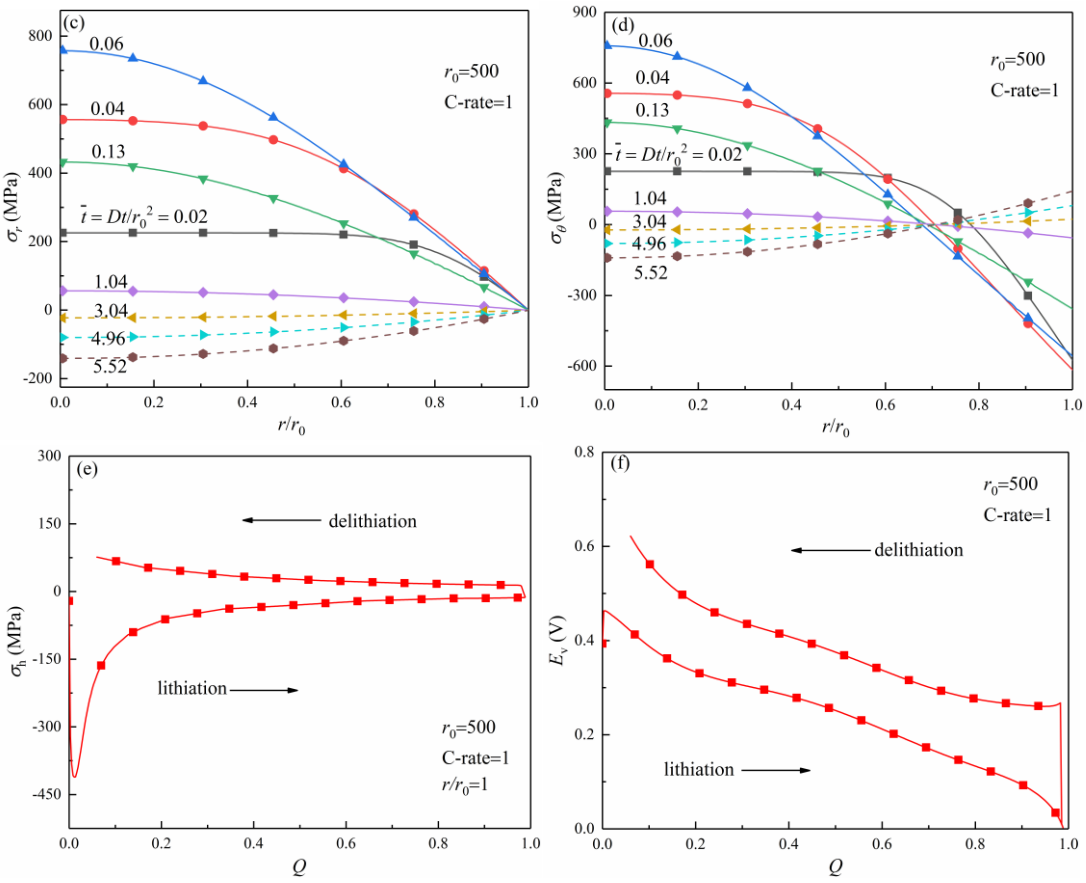

Figure 2. Spatial distributions of lithium-ion concentration at lower dimensionless capacity (a) and higher dimensionless capacity (b), radial stress (c) and hoop stress (d); the evolutions of the hydrostatic pressure (e) at the surface and the electrode potential (f) with the dimensionless capacity Q for $r_0 = 500$ nm and 1C. Solid and dotted curves with symbol denote the charge and discharge process respectively

Figure 3 describes the influence of C-rate on the lithium-ion concentration, radial stress, hoop stress, hydrostatic pressure and electrode potential during the charge and discharge. The lithium-ion concentration distribution with r/r_0 is shown in Fig. 3(a) at dimensionless time $\bar{t} = 0.08$ for different C-rate. It can be observed from Fig. 3(a) that 1) higher the C-rate leads to higher the concentration of lithium-ion at a fixed position, which means less time to reach the steady and the charge termination; 2) when the C-rate is higher, the difference of the concentration between the center and the surface is larger, which is similar to that in [7]; 3) the lithium-ion concentration is sensitive to C-rate.

Fig. 3(b) and 3(c) show the distribution of the radial and hoop stress with r/r_0 at $\bar{t} = 0.08$ for different C-rate, respectively. When the C-rate is higher, the magnitudes of the radial and hoop stress are larger, which indicates that it is easier for the electrode to destroy for higher C-rate.

The hysteresis of the hydrostatic pressure and electrode potential at different C-rates are illustrated in Fig. 3(d) and 3(e), respectively. Obviously, higher C-rate leads to larger magnitude of the hydrostatic pressure in Fig. 3(d) because the magnitudes of the radial and hoop stress are larger for higher C-rate and further they lead to larger hydrostatic pressure according to $\sigma_h = (\sigma_r + 2\sigma_\theta)/3$. Moreover, the hysteresis loop of the hydrostatic pressure between lithiation and delithiation will

become larger for higher C-rate. The variation of the hysteresis loop of the potential with the C-rate is similar to that of the hydrostatic pressure, as indicated in Fig. 3(e). That is, the hysteresis loop of the potential between lithiation and delithiation will increase when the C-rate increases, which is due to that the electrode potential deviates from the equilibrium potential more for larger C-rate and hydrostatic pressure according to Eq. (4) and Fig. 3(d). What's more, when the C-rate is larger, the electrode potential drops to a cut-off potential more quickly and the dimensionless capacity Q, at which the lithiation is terminated, is smaller. Therefore, the lower C-rate is beneficial to reduce stress and enhance the actual battery capacity.

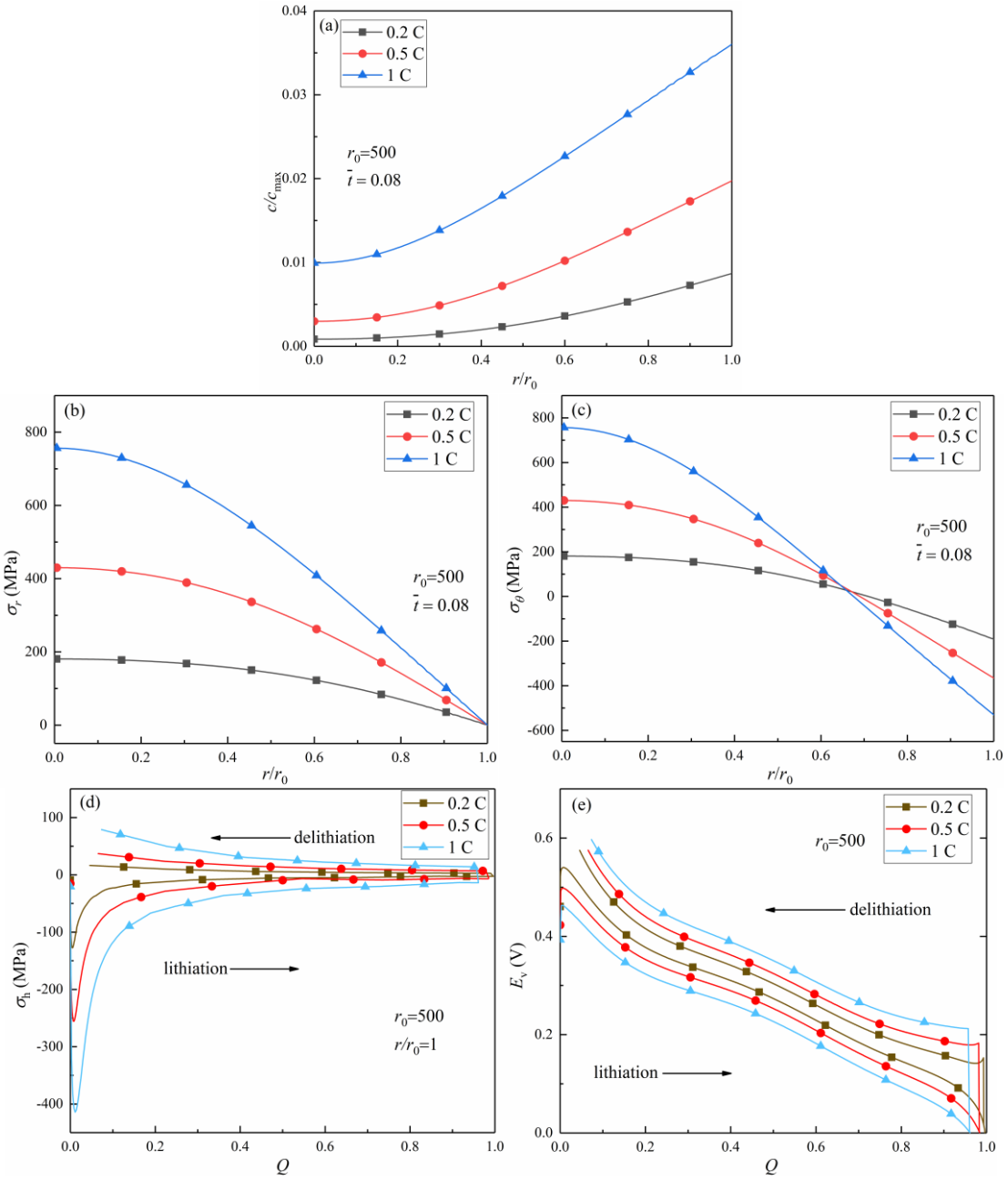

Figure 3. Spatial distributions of lithium-ion concentration (a), radial stress (b) and hoop stress (c) at $\bar{t} = 0.08$; the evolutions of the hydrostatic pressure (d) at the surface of electrode and the electrode potential (e) with the dimensionless capacity Q for different C-rate and $r_0 = 500$ nm

Figure 4 discusses the influence of electrode particle radius on the distribution of the lithium-ion concentration, radial stress, hoop stress, hydrostatic pressure and electrode potential under $n_C = 1$ C galvanostatic operation. It is noted that the time is not given by dimensionless $\bar{t}$ but $t = 100$ s in Figs. 4(a)-4(c) because dimensionless time is related to the electrode particle radius and the influence of only the radius on them is investigated at the same charge time. It can be seen from Fig. 4(a) that the lithium-ion concentration is higher for the larger particle radius, which is due to that the diffusion flux becomes larger for larger particle radius according to Eq. (15) and $i_n = n_c c_{\max} F r_0 / 10800$. Additionally, when the particle radius is smaller, it is easier to reach the steady of the lithium-ion concentration and the distribution of concentration is more homogeneous.

Fig. 4(b) and 4(c) depict the distribution of the radial and hoop stress at $t = 100$ s for different electrode particle radius during the charge, respectively. The magnitudes of the radial and hoop stresses increase with the increase of the radius, which is consistent with the result of Zhang [6]. So it is necessary to reduce the radius in order to avoid the destruction of the electrode.

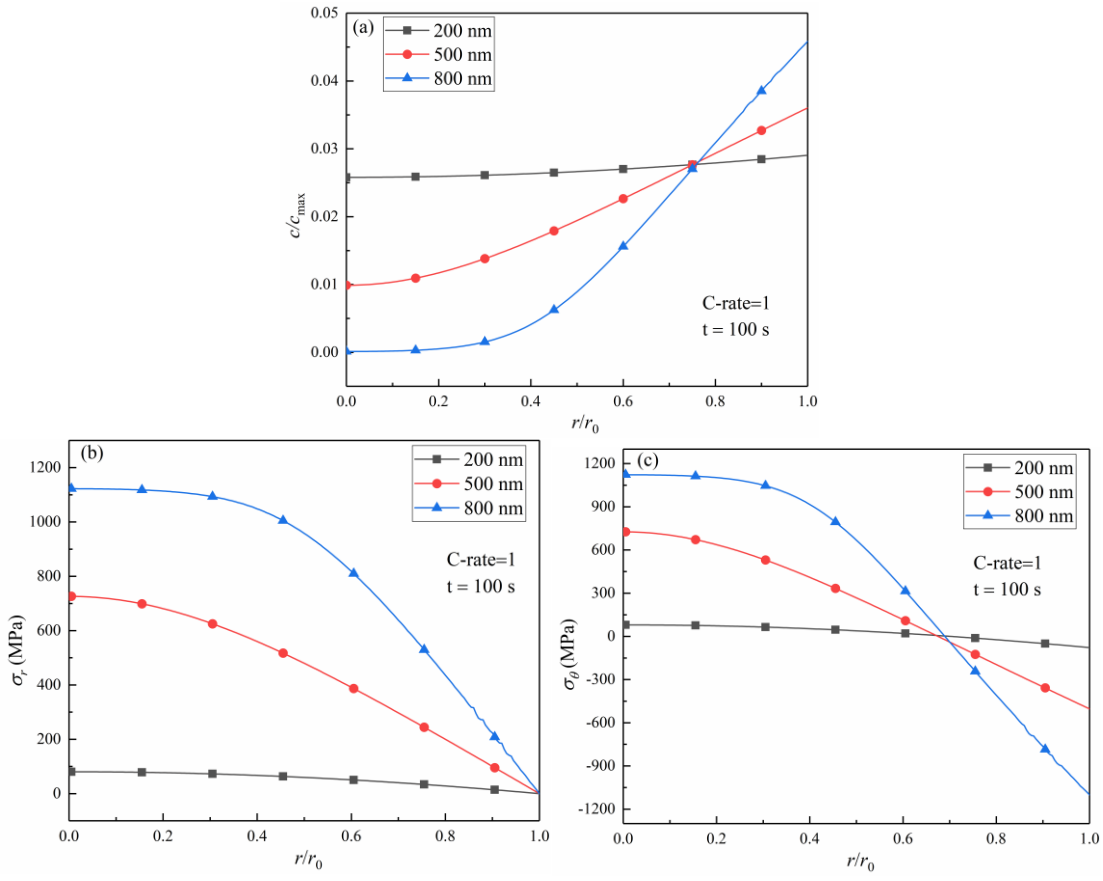

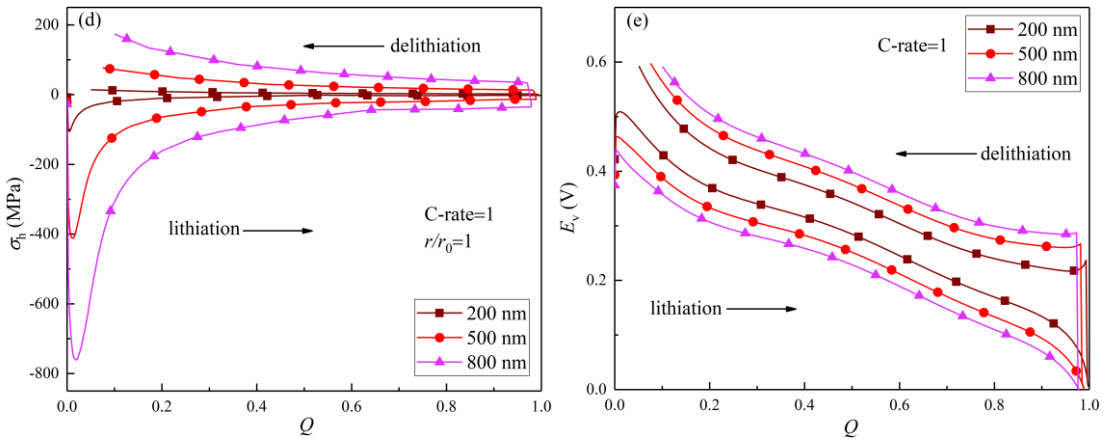

Figure 4. Spatial distribution of lithium-ion concentration (a), radial stress (b) and hoop stress (c) at $t = 100$ s; the evolution of the hydrostatic pressure (d) at the surface of electrode and the electrode potential (e) with the dimensionless capacity Q for different r_0 at 1C-rate

Fig. 4(d) and 4(e) exhibit the hysteresis of the hydrostatic pressure at the surface of electrode and the electrode potential during lithiation and delithiation, respectively. It is obvious that for a larger radius, the hydrostatic pressure is greater, which is due to the greater radial stress and the greater stress on the hoop, as shown in the figure. 4(b) and 4(c). The hysteresis loop of the hydrostatic pressure is greater for a greater radius in Fig. 4(d), and that of the electrode potential is bigger for larger radius in Fig. 4(e). Additionally, when the potential of the electrode is zero, the effective capacity Q increases as the particle size decreases. This behavior is due to the fact that the electrode potential drops to zero faster for a larger compressive stress during the lithiation process according to Eq. (4) and Fig. 4(d) when the particle radius is larger. Therefore, the large particle size and compressive stress can reduce effective capacity, consistent with [26].

In order to make clear how the stress impacts on the lithium-ion concentration and the electrode potential, the comparisons between the present model and Jin's model [17] is made in Fig. 5. The effect of the stress on the diffusion is neglected in Jin's model, and diffusion equation is described by only pure Fick's law while there exists fully coupled in this work. Fig. 5(a) and (b) are the concentration comparisons at lower SOC and higher SOC, respectively. Observed from Fig. 5(a) and (b), the distribution of lithium ion concentration along the radial direction is more uniform, as stress and electrochemical potential improve lithium ion diffusion. Fig. 5(c) is the electrode potential comparison during lithiation and delithiation. The electrode potential in the current model falls to zero slower than in the Jin model during the lithiation. When the impact of the stress on the diffusion is considered, the dimensionless capacity Q, at which the lithiation is terminated, is larger. Thus, Jin's model shortens the lithiation process however the lithiation is not finished in fact.

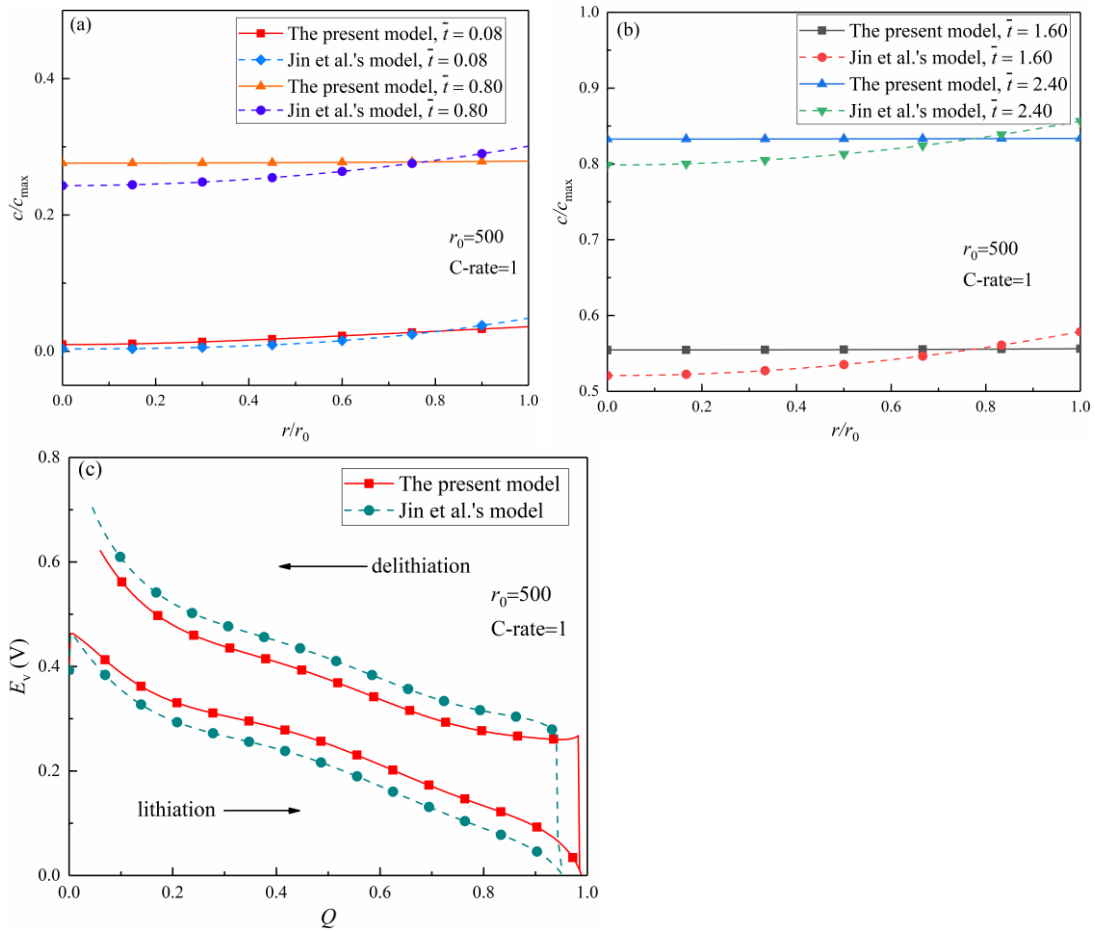

Figure 5. Comparisons of lithium-ion concentration at lower SOC (a) and higher SOC (b) and the hysteresis of electrode potential (c) between the present model and Jin's model (without the effect of the stress on the diffusion) for $r_0 = 500$ nm and 1C

4. CONCLUSIONS

Taking into account the effects of the stress on the diffusion and electrode potential, a fully coupled electro-chemo-mechanical model in the spherical electrode is developed on the basis of modified Butler-Volmer electrochemical reaction, diffusion and mechanical equilibrium equation. Numerical simulations are then carried out to examine the influence of the electrode particle radius and the C-rate on the lithium ion concentration, stress and hysteresis of the electrode potential during galvanostatic operation. Some comparisons of the lithium ion concentration and hysteresis of the electrode potential between the present model and the Jin model are carried out. Numerical results indicate that 1) the electrode particle radius and C-rate play a significant role in the mechanical stress and electric potential for silicon electrode; 2) the smaller C-rate is beneficial to reduce the diffusion-induced stress and improve the effective capacity of the battery; 3) when the particle radius is larger, the magnitude of diffusion-induced stress is larger, and the effective capacity is smaller.

ACKNOWLEDGEMENTS
The supports from State Key Laboratory for Strength and Vibration of Mechanical Structures Open Foundation of Xi'an Jiaotong University (Grant No. SV2018-KF-25), NSFC (Grants No. 11902076), Natural Science Foundation of Fujian Provincial (No. 2018J01663), Joint Fund for Tianjin and Fuzhou University (No. TF2020-2), and Scientific Research Program Funded by Fujian Provincial Education Commission (No. JT180026).

DATA ACCESSIBILITY
Data available on request from the authors. The data that support the findings of this study are available from the corresponding author upon reasonable request.

References

1. C. K. Chan, H. Peng, G. Liu, K. McIlwrath, X. F. Zhang, R. A. Huggins and Y. Cui, *Nat. Nanotechnol.*, 3(2008) 31-35.
2. J. W. Choi, D. Aurbach, *Nat. Rev. Mater*., 1(2016) 16013.
3. H. Sitinamaluwa, J. Nerkar, M. C. Wang, S. Q. Zhang and C. Yan, *RSC Adv.,* 7(2017) 13487-13497.
4. X. Gao, D. N. Fang and J. M. Qu, *Proc. R. Soc.* A, 471(2015) 20150366.
5. S. Prussin, *J. Appl. Phys*., 32(1961) 1876-1881.
6. X. C. Zhang, W. Shyy and A. M. Sastry, *J. Electrochem. Soc*., 154(2007) A910-A916.
7. K. J. Zhao, M. Pharr, J. J. Vlassak and Z. G. Suo, *J. Appl. Phys*., 108(2010) 073517.
8. Y. T. Cheng, M. W. Verbrugge, *J. Appl. Phys*., 104(2008) 083521.
9. Y. H. Suo, F. Q. Yang, *Acta Mech*., 230(2018) 993-1002.
10. H. Hu, P. F. Yu and Y. H. Suo, *Acta Mech.*, 231(2020) 2669-2678.
11. Y. Li, Q. Zhang, K. Zhang and F. Q. Yang, *J. Power Sources*, 457(2020) 228016.
12. V. A. Sethuraman, V. Srinivasan, A. F. Bower and P. R. Guduru, *J. Electrochem. Soc*., 157(2010) A1253-A1261.
13. D. M. Piper, T. A. Yersak and S. H. Lee, *J. Electrochem. Soc*., 160(2012) A77-A81.
14. B. Lu, Y. Song, Q. Zhang, J. Pan, Y. T. Cheng and J. Zhang, *Phys. Chem. Chem. Phys*., 18(2016) 4721-4727.
15. A. F. Bower, P. R. Guduru and V. A. Sethuraman, *J. Mech. Phys. Solids*, 59(2011) 804-828.
16. Y. C. Song, A. K. Soh and J. Q. Zhang, *J. Mater. Sci.*, 51(2016) 9902-9911.
17. C. J. Jin, H. L. Li, Y. C. Song, B. Lu, A. K. Soh and J. Q. Zhang, *Sci. China Technol. Sci*., 62(2019) 1357-1364.
18. J. Y. Peng, J. H. Wang, B. Shen, H. L. Li and H. M. Sun, *Acta Phys. Sin*., 68(2019) 090202. (in Chinese)
19. F. Hao, W. X. Wang and P. P. Mukherjee, *J. Electrochem. Soc*., 167(2020) 080513.
20. M. T. McDowell, I. Ryu, S. W. Lee, C. Wang, W. D. Nix and Y. Cui, *Adv. Mater*., 24(2012) 6034-6041.
21. M. Gu, H. Yang, D. E. Perea, J. G. Zhang, S. Zhang and C. M. Wang, *Nano Lett*., 14(2014) 4622-4627.
22. L. L. Luo, P. Zhao, H. Yang, B. R. Liu, J. G. Zhang, Y. Cui, G. H. Yu, S. L. Zhang and C. M. Wang, *Nano Lett.*, 15(2015) 7016-7022.
23. Y. H. Suo, F. Q. Yang, *Acta Mech. Sin*., 35(2018) 589-599.
24. J. C. M. Li, *Scr. Metall*., 15(1981) 21-28.
25. Y. J. Lu, P. L. Zhang, F. H. Wang, K. Zhang and X. Zhao, *Electrochim. Acta*, 274(2018) 359-369.

26. G. Bucci, T. Swamy, S. Bishop, B. W. Sheldon, Y. M. Chiang and W. C. Carter, *J. Electrochem. Soc*., 164(2017) A645-A654